

^8B breakup in elastic and transfer reactions

A. M. Moro* and R. Crespo

Departamento de Física, Instituto Superior Técnico, Av. Rovisco Pais, 1049-001 Lisboa, Portugal

F. Nunes

Universidade Fernando Pessoa, Praça 9 de Abril, 4200, Porto, Portugal

I. J. Thompson

Department of Physics, University of Surrey, Guildford GU2 5XH, United Kingdom

(Received 1 April 2002; published 28 August 2002)

We have studied the transfer reaction $^{14}\text{N}(^7\text{Be},^8\text{B})^{13}\text{C}$ at $E_{\text{lab}}=84$ MeV, paying special attention to the effects of the coupling to the continuum in the exit channel. Using the continuum discretized coupled channels (CDCC) formalism, we find that these effects are important for the description of the elastic scattering observables. However, for the transfer process, differences between the predictions of the differential cross section within the distorted wave Born approximation (DWBA) and the CDCC-Born approximation (CDCC-BA) are found to be negligible. This result supports the use of the DWBA method as a reliable tool to extract the $S_{17}(0)$ factor in this case.

DOI: 10.1103/PhysRevC.66.024612

PACS number(s): 24.10.Ht, 24.10.Eq, 25.55.Hp

I. INTRODUCTION

Many reaction formalisms have been developed to study stable and unstable nuclei in the last few years and applied to extract structure information from scattering processes. Often, there is an interplay between the structure information that should be extracted from the reaction data and the reaction process itself. Thus, in each case, in order to extract reliable structure information, the adequacy of the scattering formalism needs to be addressed in detail.

Of timely importance is the coupling to breakup states when the scattering process involves loosely bound nuclei. Early analysis of elastic scattering with deuterons have shown that it is important to include the couplings to the continuum [1,2]. More recently, the analysis of scattering reactions of loosely bound nuclei has progressed beyond the collective optical model (OM) approach to a more microscopic treatment (i.e., Ref. [3] for elastic, Ref. [4] inelastic, Refs. [5–8] for breakup, and Ref. [9] for transfer reactions). In these approaches, the few-body nature of the loosely bound nucleus is incorporated *ab initio* in the scattering model and the coupling to the breakup channels are either introduced explicitly [10–12], effectively through polarization potentials [13,14], or to all the orders [15,16].

The study of the coupling to the continuum in transfer processes with loosely bound nuclei is also of relevance in astrophysics. The asymptotic normalization coefficient (ANC) method [17] has been put forward as an alternative way to obtain information about the low energy S factors. This method uses the absolute normalization of a peripheral transfer reaction to determine the normalization of the vertices involved in the process. Its applicability depends crucially on the validity of the distorted wave Born approximation (DWBA) conventionally used. The main assumptions

are that the transition amplitude for the transfer can be evaluated in the Born approximation and that the incoming and outgoing elastic waves are properly described in terms of effective optical potentials. Typically, the optical potentials used in DWBA calculations are deduced from the analysis of entrance (and exit, whenever existent) elastic scattering data, to reduce the uncertainties of the ANCs extracted from the transfer [18]. The possibility of systematic errors in this method has been a source of concern [19]. As a result, several tests have been performed to ensure its validity (see, for example, a comparison with direct measurements [20] or the extraction of the same information from a set of different reactions [21]). Very recently, the importance of coupling to excited inelastic channels of the target was assessed [22] and results emphasize that care should be taken when choosing the target.

A significant number of the unmeasured capture reactions of interest in astrophysics involve nuclei on the drip line [19,23]. The proximity of threshold suggests that breakup channels may play a role in their reaction mechanism. These implications have not yet been evaluated for any of the transfer reactions used so far. A prime example is the extraction of S_{17} from $^{14}\text{N}(^7\text{Be},^8\text{B})^{13}\text{C}$ at $E_{\text{lab}}=84$ MeV [24,25].

One of the reasons for ^8B attracting much of the nuclear physics efforts is its relevance to astrophysics, namely, to the solar neutrino problem [19]. The first experiment performed with the aim of extracting an ANC for ^8B was a (d,n) reaction [26]. Meanwhile, two transfer reactions on medium mass targets were measured with the same aim: $^{10}\text{B}(^7\text{Be},^8\text{B})^9\text{Be}$ [24,27] and $^{14}\text{N}(^7\text{Be},^8\text{B})^{13}\text{C}$ [24], both at $E_{\text{lab}}=84$ MeV. The joint analysis of these reactions [28] provided an accuracy for $S_{17}(0)$ greater than that of the direct capture measurements [29]. Coupled channel estimates [22] showed that the excited states of the target can have a strong influence when the target is ^{10}B but not when ^{14}N is used. Consequently, the $S_{17}(0)$ value extracted from $^{10}\text{B}(^7\text{Be},^8\text{B})^9\text{Be}$ should not be used without further inelastic

*Electronic address: moro@romantico.us.es

studies, but the value extracted from $^{14}\text{N}(^7\text{Be}, ^8\text{B})^{13}\text{C}$ remains valid up to now. Until recently, S_{17} extracted from both the transfer reaction of Ref. [24] and the Coulomb dissociation data [30] were consistent with the direct capture measurements. However, the very recent direct capture data from Seattle [31] not only improves the accuracy but provides a $S_{17}(0)$ 30% larger than the previous values. While differences within the direct capture data sets are being understood, all sources of possible systematic errors in the analysis of the data from indirect methods need to be checked. Given that, in ^8B , the proton is bound by only 0.137 MeV, one can suspect that coupling to continuum states may play an important role in the reaction dynamics and affect the ANC results.

The aim of this work is thus to study consistently the effects of continuum couplings of ^8B , both in the elastic scattering and the transfer process. In Sec. II, we discuss the formalism used in both kinds of processes. In Sec. III we analyze the elastic scattering of $^8\text{B}+^{13}\text{C}$ and discuss the effects of coupling to the continuum in the calculated differential cross section. In Sec. IV, we analyze the transfer reaction $^{14}\text{N}(^7\text{Be}, ^8\text{B})^{13}\text{C}$ using the CDCC-BA framework: Born approximation (BA) for the transfer couplings and coupled channel continuum discretization (CDCC) for the ^8B continuum couplings. Finally in Sec. V the conclusions of the work are drawn.

II. THEORETICAL FRAMEWORK

As mentioned previously, ^8B is a weakly bound system with a breakup $p+^7\text{Be}$ threshold close to the ground state. For many purposes this nucleus can be well described by a two-cluster model in which the valence proton is coupled to a ^7Be inert core (e.g., Ref. [32]). In order to include the ^8B continuum states as intermediate steps in the elastic or transfer process, we make use of the CDCC formalism [10–12].

Consider the three-body scattering problem of a composite nucleus $A=C+v$ impinging on a stable nucleus c . The full Hamiltonian for the problem is

$$H = h_c + h_A + T_\alpha + V_\alpha, \quad (1)$$

where the Hamiltonian for the composite nucleus A is $h_A = T_{cv} + V_{cv} + h_c + h_v$ and V_α is the sum of interaction between the clusters and the stable nucleus c , $V_\alpha = V_{cC} + V_{vc}$. Let r be the vc separation, and R the projectile-target coordinate.

For simplicity, we ignore the internal spins in the notation, and consider only excitations of the projectile A . Keeping in mind the application to loosely bound nuclei, we assume that A has only one bound state. Then $h_A \phi_0(r) = \epsilon_0 \phi_0(r)$ defines the ground state wave function and $h_A \phi_{lm,k} = \epsilon_k \phi_{lm,k}$ defines the continuum states (labeled by the angular momentum l , its projection m , and the linear momentum k).

The CDCC method makes a double truncation of the continuum in both energy and angular momentum, working in the subspaces $0 \leq k \leq k_{max}$ and $0 \leq l \leq l_{max}$. Moreover, the excitation energy range is subdivided into a number of inter-

vals, usually called *bins*. For each such bin, a representative square integrable wave function is constructed by an appropriate superposition of the continuum functions inside the bin. Thus, for a total angular momentum J with projection M , the CDCC scattering wave function for the $c+A$ system is expanded as

$$\begin{aligned} \Psi_{JM}^{CDCC}(\mathbf{r}, \mathbf{R}) = & [\phi_0(\mathbf{r}) \otimes Y_L(\hat{R})]_{JM} \chi_{0,L}^J(R) \\ & + \sum_{l=0}^{l_{max}} \sum_{L=|J-l|}^{J+l} \sum_{i=1}^N \chi_{i,L}^J(R) \\ & [\phi_{i,l}(\mathbf{r}) \otimes Y_L(\hat{R})]_{JM}, \end{aligned} \quad (2)$$

with $N = k_{max}/\Delta k$. Here $\phi_{i,l}(\mathbf{r})$ are the bin wave functions; $\chi_{i,l}^J(R)$ and $\chi_{0,L}^J(R)$ are the radial wave functions for the relative motion between c and A .

The radial functions $\chi_{0,L}^J$ and $\chi_{i,l}^J$ are determined by solving a set of coupled equations in the truncated space. The coupling potentials between different channels are given by

$$V_{il:i'l'}(\mathbf{R}) = \langle \phi_{il}(\mathbf{r}) | V_\alpha(\mathbf{r}, \mathbf{R}) | \phi_{i'l'}(\mathbf{r}) \rangle, \quad (3)$$

where it is understood that $i=0$ stands for the ground state (g.s.). These coupling potentials include the g.s.-g.s matrix element (also known as the Watanabe potential), g.s.-continuum terms, and continuum-continuum couplings. The latter can be handled in the same way as the others because the continuum bins have been made square integrable. The wave function (2) permits the description of the elastic and breakup processes for the reaction $A+c$.

Let us now consider the transfer reaction $a(C,A)c$ ($a=c+v$, $A=C+v$), where we have chosen the notation such that the exit channel of the transfer corresponds to the elastic channel presented above. The prior form of the transition amplitude for the transfer reaction process is [33]

$$T_{\text{prior}} = \langle \Psi_f^{(-)} | V_{vc} + U_{cc} - U_\alpha | \chi_\alpha^{(+)} \phi_a \phi_c \rangle, \quad (4)$$

where V_{vc} is the potential that binds the v valence particle to the C core, U_{cc} is the core-core potential, and U_α is an arbitrary potential that generates the distorted wave function in the entrance channel $\chi_\alpha^{(-)}$. Note that $\Psi_f^{(-)}$ is the total exact wave function with ingoing boundary conditions. In Eq. (4), V_{vc} is a real potential, while U_α can be chosen either as real or complex.

In practice, Eq. (4) is not directly used, as it requires the knowledge of the exact solution of the three-body Schrödinger scattering equation, a rather complicated problem on its own. Approximations of this general form are developed according to the desired applications.

When the coupling between the partitions $a+C$ and $A+c$ is sufficiently weak, the transfer process can be treated in the Born approximation. Even in this situation, if the coupling to some excited states of any of the partitions is strong, the transfer process can proceed via these intermediate states. In these circumstances, it is convenient to solve the coupled equations that include the couplings between the different excited states, followed by the calculation of the transfer in the Born approximation. This procedure is known as the

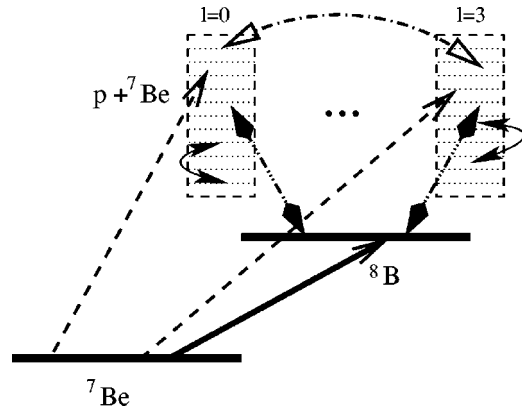


FIG. 1. Couplings included in the CDCC-BA calculation.

coupled channels Born approximation method (CCBA). When the coupling between the excited states of the same partition are weak, a further approximation is commonly performed by neglecting the explicit coupling to these states. This procedure is known as DWBA. Even when the couplings are not so weak, they may be at least partially taken into account by an appropriate choice of the optical potentials.

When weakly bound nuclei are involved, the CCBA is expected to be a reasonable approach because the transfer cross section is small due to the unfavorable Q matching. However, couplings to continuum states may still be important, as these can act as intermediate steps in the rearrangement process. It is not obvious that the DWBA approach properly accounts for these continuum effects. Nevertheless, this procedure has been used recently in the analysis of reactions involving weakly bound systems as a tool to extract the ANC information. Therefore, it is timely to perform a detailed analysis of the scattering frameworks used to describe the transfer processes. In particular, it is relevant to investigate to what extent the effects of the coupling to the continuum can be incorporated effectively in the optical potentials used by the DWBA approach.

In the case of elastic and inelastic scattering, a common procedure is to represent the continuum spectrum in $\Psi_f^{(-)}$ by a finite set of normalizable states, such as the CDCC expansion of Eq. (2). When rearrangement channels are to be considered, as in Eq. (4), since the transfer step itself is not strong we can plausibly approximate the exact wave function appearing in Eq. (4) by the CDCC wave function of Eq. (2). This procedure is called the CDCC-BA method. In CDCC-BA the exact transition amplitude is approximated by

$$T_{\text{prior}}^{\text{CDCC-BA}} = \langle \Psi_f^{\text{CDCC}(-)} | V_{vc} + U_{cc} - U_{\alpha} | \chi_{\alpha}^{(+)} \phi_a \phi_c \rangle. \quad (5)$$

All couplings included in the CDCC-BA applied to the (⁷Be,⁸B) case are schematically illustrated in Fig. 1.

Note that, since the amplitude (5) is only approximate, the potential U_{α} is no longer arbitrary. Thus, the transfer amplitude calculated by means of Eq. (5) depends on the choice of this potential. In analogy to what is commonly done in

coupled channel analysis, we take $U_{\alpha} = U_{ac}$, i.e., the optical potential that reproduces the elastic scattering in the entrance channel.

Our choice of the prior representation for the transfer matrix element is not arbitrary. In the post form, the binding interaction is that of the exiting projectile V_{vc} and the remnant term is the difference between the core-core interaction U_{cc} and the optical potential for the exit channel $U_{\beta} = U_{ca}$. However, this exit channel optical potential is often unknown; contrary to the entrance channel elastic data, elastic scattering in the exit channel cannot be measured in the same experiment, and in many cases it is just unmeasurable as both the projectile and the target are radioactive. It can then be found either by fitting the scattering from the CDCC model, or by extrapolating from neighboring nuclei. The prior form of the CDCC-BA approach, by contrast, does not require any knowledge of the optical potential U_{β} for this exit channel. It seems more appropriate, therefore, to use the prior form representation of the transition operator and, consequently, all the calculations presented hereafter were performed in this representation.

The further approximation of the CDCC by just its elastic channel, found with some optical potential U_{β} , gives the DWBA transition amplitude in the prior form:

$$T_{\text{prior}}^{\text{DWBA}} = \langle \chi_{\beta}^{(-)} \phi_a \phi_c | V_{vc} + U_{cc} - U_{ac} | \chi_{\alpha}^{(+)} \phi_a \phi_c \rangle. \quad (6)$$

This simple approximation, very commonly used in ANC analyses, still requires knowledge of the optical potential for the exit channel U_{ac} , and hence suffers from the difficulties enumerated above. However, if the transfer cross sections are not very sensitive to this potential, then the DWBA will still be a useful procedure. We examine this sensitivity below, by studying the degree of agreement between the DWBA and the CDCC. In both approaches, the remnant term of the transition matrix element for systems where a nucleon is transferred from a well bound state to a loosely bound state (or vice versa) is often not negligible and should be properly accounted for.

III. THE ELASTIC SCATTERING ⁸B+¹³C

We investigate in this section the elastic scattering ⁸B + ¹³C at $E_{\text{lab}} = 78.4$ MeV, which is the exit channel in the transfer reaction that we wish to analyze in the present work. In particular, we study the importance of the continuum in the calculated differential cross section. This reaction was previously analyzed in Ref. [25] using a renormalized double-folding (RDF) potential obtained by an analysis of nearby stable nuclei. A parametrization of this RDF potential in terms of the usual Woods-Saxon forms was also derived by fitting the outer part of the RDF potential. Since these fitted potentials may differ in the inner part from the original RDF potentials, we used the latter in our calculations, as in the results presented in Ref. [25]. As this interaction is derived from a systematic study on stable nuclei, it is not clear how adequate are these extrapolations to loosely bound nuclei. Elastic data for ⁸B+¹³C would help to shed light on these issues.

TABLE I. Parameters of the potentials used in this work. Depths are expressed in MeV and radii and diffuseness in fm. The first three rows correspond to optical potentials and the last two rows are the binding potentials. Reduced radii are to be multiplied by $A_p^{1/3} + A_T^{1/3}$ for nucleus-nucleus scattering and by $A_T^{1/3}$ for nucleon-nucleus scattering.

System	V	V_{so}	r_V	a_V	W_V	W_S	r_W	a_W	r_C	Ref.
${}^7\text{Be} + {}^{13}\text{C}$ (1)	54.3		0.92	0.79	29.9		1.03	0.69	1.	[25]
${}^7\text{Be} + {}^{13}\text{C}$ (2)	99.8		0.77	0.81	22.0		1.01	0.81	1.	[25]
$p + {}^{13}\text{C}$	60.4		1.14	0.57		5.8	1.14	0.50	1.25	[34]
$p + {}^7\text{Be}$	44.7	4.9	1.25	0.52					1.25	[32]
$p + {}^{13}\text{C}$	51.4		1.30	0.65					1.30	

In this section we analyze the same reaction in terms of the CDCC formalism for two reasons. First, this treatment allows an explicit study of the role of the continuum, and second, it provides an alternative analysis to the RDF that does not require the optical potential for ${}^8\text{B} + {}^{13}\text{C}$, thus providing a valuable reference in the absence of experimental data.

An important ingredient of the CDCC calculation is the bound state wave function of the ${}^8\text{B}$ nucleus. For the binding potential, we have adopted the parameters given in Ref. [32] and listed in Table I. The valence proton wave function is considered to be a pure $p_{3/2}$ configuration coupled to a zero-spin core of ${}^7\text{Be}$ with unit spectroscopic factor. Although it is known that there is a $p_{1/2}$ that has a small contribution to the cross section [24], we chose to neglect it to make the CDCC calculations feasible.

The interaction between the projectile ${}^8\text{B}$ and the target ${}^{13}\text{C}$ to be used in the CDCC calculation is written as the sum of the interactions $U({}^7\text{Be}, {}^{13}\text{C})$ and $U(p, {}^{13}\text{C})$. No experimental data for the elastic scattering ${}^7\text{Be} + {}^{13}\text{C}$ at the relevant energies (≈ 68 MeV) have been found in the literature. Nevertheless, the similarity in the structure of ${}^7\text{Be}$ and its mirror partner ${}^7\text{Li}$ suggests to describe this reaction using the potential taken from the reaction ${}^7\text{Li} + {}^{13}\text{C}$, for which experimental data exists at 63 MeV. The $U(p, {}^{13}\text{C})$ was taken from nucleon-nucleus global parametrizations.

Convergence of the CDCC results was achieved with a matching radius of 40 fm and a maximum total angular momentum of $L_{\text{max}} = 100$. The continuum spectrum was divided into $N = 10$ bins of equal energy width in the range from 0 to 9 MeV. We took into account s , p , and d continuum partial waves. All the calculations were performed with the computer code FRESKO [35].

We checked the sensitivity of the calculation with respect to the $U({}^7\text{Be}, {}^{13}\text{C})$ and $U(p, {}^{13}\text{C})$ interactions. To analyze the uncertainty associated with the interaction $U(p, {}^{13}\text{C})$, we compare in Fig. 2(a) the calculated differential cross section for the $p + {}^{13}\text{C}$ elastic scattering (as ratio to Rutherford), using several proton- ${}^{13}\text{C}$ interactions, adopted from the global parametrizations of Watson *et al.* [34], represented by the solid curve, Becchetti and Greenless [36] (dashed line), and Perey [37] (dashed dotted line). In all three cases the spin-orbit term was omitted.

The calculated CDCC elastic angular distributions shown in Fig. 2(b) with the Watson and Perey parametrizations are very similar, but significantly different from that calculated

with the Becchetti-Greenless potential.

As is well known, the Becchetti-Greenless parameterization is better suited for medium mass and heavy mass nuclei, and for higher scattering energies. Thus, the use of this optical potential to describe the scattering of $p + {}^{13}\text{C}$ around 10 MeV may be questionable. This, together with the fact that the Watson and Perey parametrizations provide essentially the same elastic scattering, suggests that we can use either of these with some confidence. From hereafter, the Watson potential of Ref. [34] will be used in all the CDCC calculations.

We study now the sensitivity of the calculated differential cross sections with respect to the $U({}^7\text{Be}, {}^{13}\text{C})$ potential. Figure 3(a) shows the calculated elastic scattering cross section for ${}^7\text{Be} + {}^{13}\text{C}$ using the potentials Pot1 (solid curve) and Pot2 (dashed-dotted curve) from the reaction ${}^7\text{Li} + {}^{13}\text{C}$ at 63 MeV analyzed in Ref. [25] and listed in Table I. Also included in Fig. 3(a) is the result obtained with the optical potential $U({}^7\text{Be}, {}^{14}\text{N})$ (dashed line). In Fig. 3(b) we show the corresponding CDCC calculations for the ${}^8\text{B} + {}^{13}\text{C}$ elastic scattering at 78.4 MeV. It is observed that the CDCC calculations for ${}^8\text{B} + {}^{13}\text{C}$, using potentials Pot1 and Pot2, give very similar results, whereas when the core-target potential is taken to be $U({}^7\text{Be}, {}^{14}\text{N})$, a somewhat bigger difference is encountered beyond 30 deg. In the following, we will use Pot1 as the core-target interaction.

Finally, we compare in Fig. 4 the CDCC (thick solid line) and pure OM calculations. The thin solid line is the OM

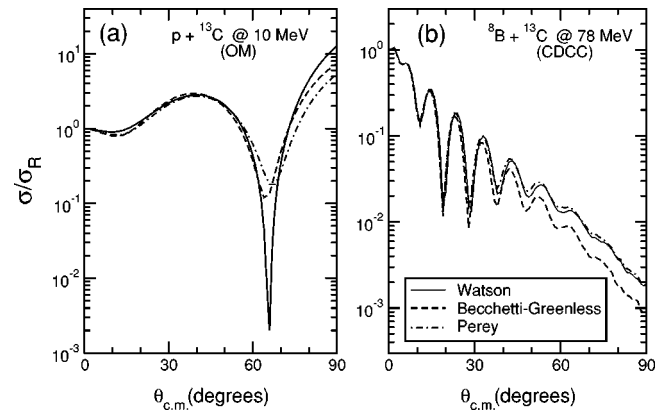


FIG. 2. (a) $p + {}^{13}\text{C}$ differential elastic cross section for different optical potentials. (b) CDCC differential elastic cross section angular distribution for ${}^8\text{B} + {}^{13}\text{C}$ at 78 MeV using different parametrizations for the $p + {}^{13}\text{C}$ interaction.

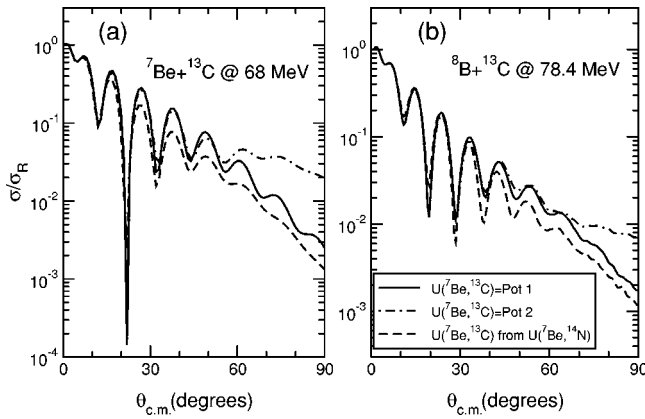


FIG. 3. (a) Calculated differential cross section angular distribution for $^7\text{Be} + ^{13}\text{C}$ at 68.6 MeV within the optical model formalism using different potential parametrizations. (b) Corresponding CDCC elastic scattering for $^8\text{B} + ^{13}\text{C}$ at 78.4 MeV.

calculation using the RDF potential derived in Ref. [25]. This agrees very well with the CDCC at small angles (up to 25 deg), but presents significant discrepancies beyond this range. Also included in this figure is an OM calculation using the same double-folding potential, but fitting the real and imaginary renormalization constants to approximate the CDCC result. We found that a value of $N_r = 0.427$ and $N_i = 0.883$ (dotted-dashed line) provides an excellent agreement between both calculations, in contrast to the value $N_r \approx 0.366$ (thin solid line) proposed in Ref. [25]. Any experimental result for this reaction at $\theta > 30$ deg would help clarify the adequacy of global parametrizations for loosely bound nuclei.

We have also estimated the effect of the ^8B continuum on the calculated elastic scattering cross section. To this end we compare in Fig. 5 the elastic differential cross section using

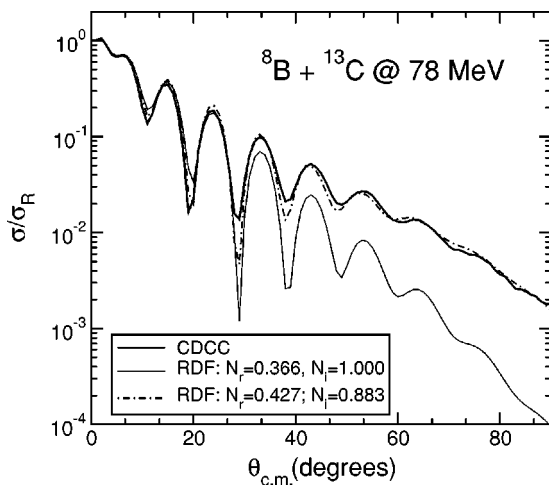


FIG. 4. Elastic cross section angular distribution (as ratio to Rutherford cross section) calculated in the CDCC framework (thick solid line) and renormalized double folding with the real renormalization constant proposed in Ref. [25] (thin solid line) and with renormalization constant adjusted to fit the CDCC (dotted-dashed line).

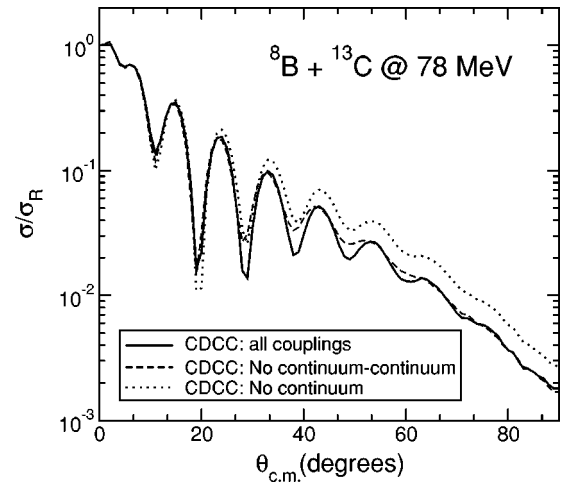


FIG. 5. Effect of the continuum in $^8\text{B} + ^{13}\text{C}$ elastic scattering at 78 MeV. The dotted line is the Watanabe calculation (i.e., the CDCC calculation without g.s.-continuum couplings). The dashed line is the CDCC with g.s.-continuum couplings, but no continuum-continuum couplings. The solid line is the full CDCC calculation with both g.s.-continuum and continuum-continuum couplings.

the full CDCC calculation (thick solid line) with a calculation in which all couplings with continuum states have been ignored (dotted line). The latter is equivalent to an optical model calculation in which the projectile-target interaction is described in terms of the Watanabe folding potential. Also represented is the CDCC without continuum-continuum couplings (dashed line). It can be seen that this truncated calculation provides cross sections that are already very close to those produced by the full CDCC calculation, suggesting that multistep processes coupling different continuum states are not very relevant in this reaction. The main CDCC effect appears to be a reduction of the cross sections caused by absorption due to breakup at near-grazing collisions.

IV. THE TRANSFER REACTION $^{14}\text{N}(^7\text{Be}, ^8\text{B})^{13}\text{C}$

We analyze in this section the transfer reaction $^{14}\text{N}(^7\text{Be}, ^8\text{B})^{13}\text{C}$ at 84 MeV, within the DWBA and CDCC-BA approaches. In order to make a reliable comparison between both formalisms we have calculated the transition amplitudes in Eqs. (6) and (5) using the same core-core interaction U_{cc} , and we take Pot1 from Table I. For the binding potential (V_{vc}) of $p + ^{13}\text{C}$ we used the parameters listed in Table I. The entrance channel was described in terms of the numerical RDF potential derived in Ref. [25]. The DWBA calculation requires also the exit optical potential $U_\beta = U(^8\text{B}, ^{13}\text{C})$, which we also took from Ref. [25] in numerical form.

The ground state and continuum structure of ^8B needed for the CDCC calculation was taken to be the same as the one in the preceding section. The ^{14}N ground state was described as a proton in a $p_{1/2}$ configuration, with a spectroscopic factor of 0.604 [24]. For the purpose of comparing the present calculations with the data we have renormalized all the calculated transfer cross sections by the spectroscopic factor $S_{p_{3/2}} = 0.737$. This value was derived from the ANC

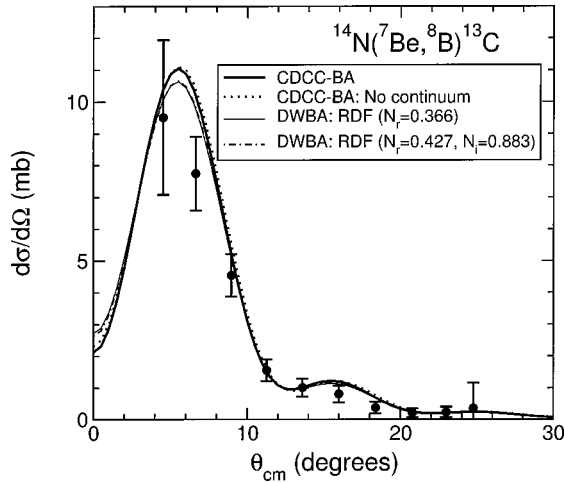


FIG. 6. Calculated transfer cross section angular distribution for the reaction $^{14}\text{N}(^7\text{Be}, ^8\text{B})^{13}\text{C}$ at 84 MeV. The thick solid line corresponds to the full CDCC-BA calculation. The dotted line is the CDCC-BA calculation without g.s.-continuum couplings. The thin solid line is the DWBA calculation using the RDF optical potential for exit channel with $N_r=0.366$. The dotted-dashed line is the DWBA calculation with the same RDF potential, but with the complex renormalization constants $N_r=0.427$ and $N_i=0.883$. All the CDCC-BA calculations include the factor $5/16$ to account for the physical nuclei spins, as discussed in Sec. IV.

reported in Ref. [24] for the $p_{3/2}$ configuration in the ^8B ground state ($C_{p_{3/2}}^2=0.371\text{ fm}^{-1}$) and the calculated asymptotic normalization constant for the single-particle orbital. All ^8B continuum couplings are taken into account, but no transfer back couplings are included, as this would worsen the fit to the elastic scattering in the entrance channel.

Note also that our simplified description of ^8B in terms of a proton coupled to a zero-spin core provides a cross section which, after multiplication of the factor $(2I_A+1)(2I_C+1)/(2I_a+1)(2I_c+1)$, is equivalent [38] to the cross section calculated with correct spins.

The resulting transfer cross sections are presented in Fig. 6. The thick solid line corresponds to the full CDCC-BA calculation. The thin solid line represents the DWBA calculation with a RDF potential for the entrance and exit channels, using $N_r=0.366$ for the two potentials. The resulting angular distribution is very close to the CDCC calculation, differing by only 5% at the maximum of the distribution, which is unmeasurable within the present experimental accuracy.

We stress, however, that as shown in the preceding section, OM and CDCC give different predictions for the elastic scattering in the exit channel at large angles. Under the circumstances, we believe that the CDCC predictions for the elastic $^8\text{B}+^{13}\text{C}$ is more reliable (see discussion in Sec. III). Notwithstanding, we have shown that these coupling effects can be easily included in the optical potential by adjusting the renormalization constants. We have then performed a DWBA calculation using the RDF with complex renormalization constants $N_r=0.427$, and $N_i=0.883$, accurately re-

producing the CDCC elastic predictions (dot-dashed line in Fig. 6). Despite the fact that this change in the renormalization constants modifies significantly the elastic cross sections of the exit channel beyond 30° , the resulting transfer cross section remains basically unaltered up to 25° , the angular range used in Ref. [24] to extract the ANC information. This result seems to support the peripheral nature of this reaction. Also shown in the figure is the calculated transfer cross section without continuum couplings (dotted line). This appears to be very similar to the full CDCC calculation. The similarity between all curves demonstrates the minor role played by the continuum of ^8B and confirms the DWBA formalism as an adequate tool to extract the ANC in this reaction, as done in Ref. [24].

In order to check the dependence of this result with the bombarding energy, we compared the CDCC and DWBA at other energies. We found that the effect of the continuum decreases as the incident energy increases. For instance, at 160 MeV the transfer cross sections calculated in CDCC-BA and DWBA differ by less than 1% at angles up to 30° . By contrast, at 40 MeV differences of around 8% were found at the maximum of the angular distribution.

V. CONCLUSIONS

In summary, we have studied the reaction $^{14}\text{N}(^7\text{Be}, ^8\text{B})^{13}\text{C}$ at 84 MeV, placing special stress on the importance of the continuum of ^8B in the description of the exit channel and in the transfer process. This reaction has been recently measured and analyzed within the DWBA formalism [24], in order to extract the astrophysical S_{17} factor for the capture reaction $^7\text{Be}+p\rightarrow^8\text{B}$. The validity of this procedure relies on the assumption that the transfer reaction occurs in one step and, also, that the entrance and exit channels are well described by optical potentials.

The importance of the ^8B continuum in the reaction mechanism has been analyzed by describing the $^8\text{B}+^{13}\text{C}$ scattering in terms of $p+^{13}\text{C}$ and $^7\text{Be}+^{13}\text{C}$ optical potentials and discretizing the ^8B continuum into energy bins. The elastic cross sections given by the CDCC solution has been compared with those obtained in the optical model analysis performed in Ref. [25]. In this reference, the elastic scattering of $^8\text{B}+^{13}\text{C}$ was analyzed in terms of a double-folding optical potential, using a renormalization constant derived from a systematic analysis of several reactions involving stable nuclei in the same energy and mass region. We found that the calculated differential elastic cross section is very similar in both approaches at forward angles, but they differ significantly at larger angles. This result casts doubt on the extrapolation of the global optical potentials derived from stable nuclei to loosely bound nuclei. Interestingly, in this reaction the CDCC effects can be accounted for very well by correcting the normalization of the double folding potential. The calculated CDCC wave function is then used in the expression for the transfer amplitude. Despite the discrepancies on the elastic scattering of the exit channel at large angles, the calculated transfer cross sections are very similar in the DWBA and CDCC-BA approaches below 25° , which was the angular range used to extract the ANC for this reaction.

Taking into account the result of Ref. [22] where coupling to excited (bound) states was also found to be negligible, to the accuracy of the present transfer data, the present analysis supports the validity of the DWBA method as a reliable tool to extract the S factor from the $^{14}\text{N}(^7\text{Be}, ^8\text{B})^{13}\text{C}$ reaction at the studied energy. Consequently, these higher order corrections to the DWBA cannot justify the disagreement between the S_{17} extracted using the ANC method and the new direct results from Seattle [31].

Similar checks for other reactions that involve loosely bound nuclei are under way. As the structure of ^8B was simplified, some interference effects could not be probed in this work. Although less important when continuum coupling

effects are small, these effects should generally be properly included. This problem is also being addressed.

ACKNOWLEDGMENTS

We are deeply grateful to J. Gómez-Camacho for his fruitful comments, and to L. Trache for providing the data, the numerical optical potentials, and other details concerning the analysis of the data presented. Support from Fundação para a Ciência e a Tecnologia (F.C.T.) under Grant No. SAPIENS/36282/99 and EPSRC under Grant No. GR/M/82141 is acknowledged. One of the authors (A.M.M.) acknowledges an F.C.T. post-doctoral grant.

-
- [1] R. C. Johnson and P. J. R. Soper, *Phys. Rev. C* **1**, 976 (1970).
 [2] S. Watanabe, *Nucl. Phys.* **8**, 484 (1958).
 [3] R. C. Johnson, J. S. Al-Khalili, and J. A. Tostevin, *Phys. Rev. Lett.* **79**, 2771 (1997).
 [4] R. Crespo and I. J. Thompson, *Nucl. Phys.* **A689**, 559c (2001).
 [5] C. A. Bertulani, L. F. Canto, and M. S. Hussein, *Phys. Lett. B* **353**, 413 (1995).
 [6] J. A. Tostevin, S. Rugmai, and R. C. Johnson, *Phys. Rev. C* **57**, 3225 (1998).
 [7] F. M. Nunes and I. J. Thompson, *Phys. Rev. C* **59**, 2652 (1999).
 [8] J. A. Tostevin, F. M. Nunes, and I. J. Thompson, *Phys. Rev. C* **63**, 024617 (2001).
 [9] N. K. Timofeyuk and R. C. Johnson, *Phys. Rev. C* **59**, 1545 (1999).
 [10] M. Yahiro, N. Nakano, Y. Iseri, and M. Kamimura, *Prog. Theor. Phys.* **67**, 1464 (1982).
 [11] M. Yahiro, Y. Iseri, H. Kameyama, M. Kamimura, and M. Kawai, *Prog. Theor. Phys. Suppl.* **89**, 32 (1986).
 [12] N. Austern, Y. Iseri, M. Kamimura, M. Kawai, G. Rawitscher, and M. Yahiro, *Phys. Rep.* **154**, 125 (1987).
 [13] M. V. Andrés, J. Gómez-Camacho, and M. A. Nagarajan, *Nucl. Phys.* **A579**, 273 (1994).
 [14] M. V. Andrés, J. Gómez-Camacho, and M. A. Nagarajan, *Nucl. Phys.* **A583**, 817 (1995).
 [15] R. Crespo and R. C. Johnson, *Phys. Rev. C* **60**, 034007 (1999).
 [16] A. M. Moro, J. A. Caballero, and J. Gómez-Camacho, *Nucl. Phys.* **A695**, 143 (2001).
 [17] H. M. Xu, C. A. Gagliardi, R. E. Tribble, A. M. Mukhamedzhanov, and N. K. Timofeyuk, *Phys. Rev. Lett.* **73**, 2027 (1994).
 [18] J. C. Fernandes, R. Crespo, F. M. Nunes, and I. J. Thompson, *Phys. Rev. C* **59**, 2865 (1999).
 [19] E. G. Adelberger *et al.*, *Rev. Mod. Phys.* **70**, 1265 (1998).
 [20] C. A. Gagliardi *et al.*, *Phys. Rev. C* **59**, 1149 (1999).
 [21] J. C. Fernandes, R. Crespo, and F. M. Nunes, *Phys. Rev. C* **61**, 064616 (2000).
 [22] F. M. Nunes and A. M. Mukhamedzhanov, *Phys. Rev. C* **64**, 062801(R) (2001).
 [23] *Nuclei in the Cosmos V, International Symposium on Nuclear Astrophysics* edited by N. Pratzos and S. Harrisopulos (Editions Frontières, Paris, 1998).
 [24] A. Azhari, V. Burjan, F. Carstoiu, C. A. Gagliardi, V. Kroha, A. M. Mukhamedzhanov, X. Tang, L. Trache, and R. E. Tribble, *Phys. Rev. C* **60**, 055803 (1999).
 [25] L. Trache, A. Azhari, H. L. Clark, C. A. Gagliardi, Y. W. Lui, A. M. Mukhamedzhanov, R. E. Tribble, and F. Carstoiu, *Phys. Rev. C* **61**, 024612 (2000).
 [26] W. Liu *et al.*, *Phys. Rev. Lett.* **77**, 611 (1996).
 [27] A. Azhari, V. Burjan, F. Carstoiu, H. Dejbakhsh, C. A. Gagliardi, V. Kroha, A. M. Mukhamedzhanov, L. Trache, and R. E. Tribble, *Phys. Rev. Lett.* **82**, 3960 (1999).
 [28] A. Azhari, V. Burjan, F. Carstoiu, C. A. Gagliardi, V. Kroha, A. M. Mukhamedzhanov, F. M. Nunes, X. Tang, L. Trache, and R. E. Tribble, *Phys. Rev. C* **63**, 055803 (2001).
 [29] F. Hammache *et al.*, *Phys. Rev. Lett.* **86**, 3985 (2001).
 [30] B. Davids, S. M. Austin, D. Bazin, H. Esbensen, B. M. Sherrill, I. J. Thompson, and J. A. Tostevin, *Phys. Rev. C* **63**, 065806 (2001).
 [31] A. R. Junghans, E. C. Mohrmann, K. A. Snover, T. D. Steiger, E. G. Adelberger, J. M. Casandjian, H. E. Swanson, L. Buchmann, S. H. Park, and A. Zyuzin, *Phys. Rev. Lett.* **88**, 041101 (2002).
 [32] H. Esbensen and G. F. Bertsch, *Nucl. Phys.* **A600**, 37 (1996).
 [33] G. R. Satchler, *Direct Nuclear Reactions* (Oxford University Press, New York, 1983).
 [34] B. A. Watson, P. P. Singh, and R. E. Seguel, *Phys. Rev.* **182**, 977 (1969).
 [35] I. J. Thompson, *Comput. Phys. Rep.* **7**, 167 (1988).
 [36] F. D. Becchetti and G. W. Greenlees, *Phys. Rev.* **182**, 1190 (1969).
 [37] C. M. Perey and F. G. Perey, *Phys. Rev.* **132**, 755 (1963).
 [38] In the absence of spin dependent forces, the transfer cross section for $^{14}\text{N}+^7\text{Be}(0^+) \rightarrow ^{13}\text{C}+^8\text{B}(3/2^-)$ should equal the sum of the cross sections $\Sigma_I ^{14}\text{N}+^7\text{Be}(3/2^-) \rightarrow ^{13}\text{C}+^8\text{B}(I)$, for $I=0^+, 1^+, 2^+, 3^+$ that result from the coupling of $I(^7\text{Be})$ to the $p_{3/2}$ proton single particle state. The physical process measured is only $^{14}\text{N}+^7\text{Be}(3/2^-) \rightarrow ^{13}\text{C}+^8\text{B}(2^+)$. According to detailed balance, one can conclude that the weight of this reaction relative to the total sum is $(2I_A+1)(2I_C+1)/(2I_A+1)(2I_C+1)=5/16$. This means that the calculated transfer cross section using a simplified description with zero spin for ^7Be needs to be multiplied by this factor.